AN IMPROVED METHOD FOR CHARACTERIZING REFLECTOR SPECULARITY FOR PARABOLIC TROUGH CONCENTRATORS

Randy Gee[1], Randy Brost[2], Guangdong Zhu[3], and Gary Jorgensen[4]

[1] Chief Technology Officer, SkyFuel, Inc. 18300 West. Highway 72, Arvada, CO 80007 USA,
Randy.Gee@skyfuel.com, 303.330.0276
[2] VP of Adv. Product Develop., SkyFuel, Inc. 10701 Montgomery Blvd. NE, Suite A, Albuquerque, NM
[3] Senior Engineer, SkyFuel, Inc. 10701 Montgomery Blvd. NE, Suite A, Albuquerque, NM 87111 USA
[4] Principal Scientist, National Renewable Energy Laboratory, 1617 Cole Blvd., Golden, CO 80401 USA

Abstract

A comprehensive analysis of the impact that reflector specularity has on the optical performance of parabolic trough solar collectors shows that beam spread from commercially available metalized polymer films results in a loss of approximately 1.5% for state-of-the-art parabolic troughs. This 1.5% loss contrasts markedly with the 5% loss indicated in a DLR-authored paper from SolarPACES 2009. The primary reason for this difference is that the former analysis did not account for the combined effect of the other optical errors in a parabolic trough system. To get accurate results, reflector specularity should be analyzed as just one factor in the optical system as a whole. It is also shown that the performance impact can be higher or lower than the 1.5%, depending on the concentration ratio of the trough concentrator being considered and the magnitude of the other optical errors of the parabolic trough solar collector.

The analysis also indicates that reflector surfaces can be accurately characterized with two fundamental quantities: a) $\rho_{2\pi}$, the solar-weighted hemispherical reflectance, and b) σ_{spec}, the rms of the reflected light distribution which is sometimes best represented as the combination of two Gaussian distributions. By describing the distribution of specularly reflected light, σ_{spec} can be used in combination with $\rho_{2\pi}$ to quantitatively, and fairly, compare various parabolic trough reflector surfaces in a way that incorporates the important system-level effects.

Keywords: specularity, specular reflectance, polymer film reflector, ReflecTech, parabolic trough

1. Introduction

A variety of reflective materials are used with parabolic trough concentrators: silvered glass, metalized polymer films, and polished and anodized aluminum with coatings that increase reflectance and improve durability. To be of practical use for solar applications, these reflectors must have high reflectance across the solar spectrum and also reflect with a high level of specularity. Both of these reflector characteristics are important, but the significance of specularity is sometimes mischaracterized and overstated for parabolic troughs. For example, there is some current discussion about a proposed standard for characterizing and comparing solar reflectors, but that method [1] is based on the assumption that all light reflected outside of a 25 mrad acceptance angle is lost, without consideration of the optical system as a whole. The result of this method is that polymer films are penalized 5% due to reduced specularity, a conclusion that is inconsistent with prior technical work [2, 3], and would make achieving high optical efficiency virtually impossible with the use of polymer films. Indeed a 5% performance penalty with polymer films is at odds with the measured optical efficiencies of parabolic troughs that use silvered films [4, 5], which are comparable with the optical efficiencies reported for troughs that use silvered glass mirrors [6, 7].
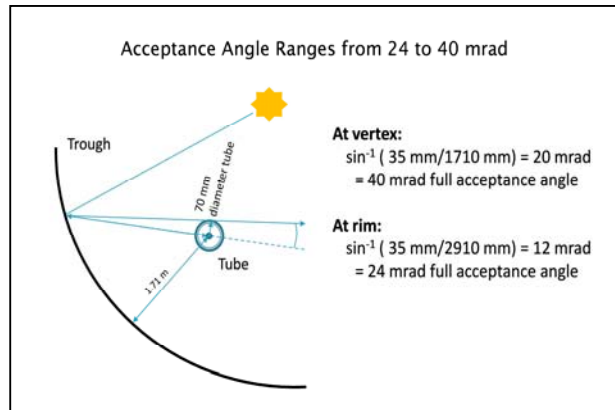

Fig. 1. Acceptance Angles for LS-3

As shown in Figure 1, the acceptance angle of a typical state-of-the-art parabolic trough (e.g. the widely used LS-3 geometry) covers the range from 24 to 40 mrads. The LS-3 geometry has a 5.76 meter aperture width and a 70 mm diameter absorber tube, which results in a concentration ratio of 82:1, when calculated as the ratio of concentrator aperture width to absorber tube diameter[1]. At the vertex of the parabolic trough, the acceptance angle is 40 mrad. At the rim, the acceptance angle is 24 mrad because of the longer distance from this outer edge of the reflector to the absorber tube.

Given this range in acceptance angles, there is no "best" acceptance angle to use when measuring specular reflectance. Further, the important issue is how effective the reflective surface is at redirecting sunlight to the optical target, a cylindrical receiver in the case of a parabolic trough. To answer this question properly, the size of the target (i.e. absorber tube diameter), and the beam spreading caused by other optical errors must be taken into account. These include concentrator slope errors, receiver placement errors, tracking errors, the finite size of the sun, and twist/misalignment along the length of the collector, etc. On one hand, there is no point in counting that a reflected light ray will hit the absorber tube if it is likely to miss the absorber because of the combined effects of other optical errors. On the other hand, there is no point in having super–specular reflector surfaces when the optical system is limited by beam spreading caused by the finite size of the sun, as well as a host of other optical effects, like slope error, that generally have a larger impact on beam spreading. Given all these considerations, we conclude that a singular measurement of reflectance at any one specific acceptance angle is insufficient.

An instrument that provides useful specularity information is the Devices & Services Model 15R portable specular reflectometer. This instrument (shown in Figure 2) has been widely used to measure reflectance for acceptance angles of 7, 15, 25 and 46 mrads. This more than covers the range of interest, and also offers a means to characterize the distribution of scattered light from any given reflector surface in an especially useful way, as described in the next section.

Fig. 2. Specular Reflectometer

2. Specularity of Silvered Polymer Reflectors

Specular reflectance (ρ_s) is the amount of light reflected into a specified acceptance angle. Alternately, it is the hemispherical reflectance ($\rho_{2\pi}$) minus the light scattered outside a specified acceptance angle, Θ. The level of specular reflectance can be expressed as a function of $\rho_{2\pi}$ and the half-width standard deviation (σ) of the distribution of the reflected light. For reflective films and polished/anodized aluminum mirrors, the reflected light distribution is usually best represented as two Gaussians, one with a generally high intensity that is highly specular (low σ) and the other having a relatively lower intensity and broader peak (high σ) [8]. The relative weight of the two Gaussians is described by the coefficient K.

$$\rho_S (\Theta) = \rho_{2\pi} \{1 - K \exp [-(\Theta/2)^2 / (2\ \sigma_1^2)] - (1-K) \exp [-(\Theta/2)^2 / (2\ \sigma_2^2)]\} \qquad (1)$$

We have taken measurements using a Model 15R D&S specular reflectometer to characterize the specularity of ReflecTech® Mirror Film, a silvered polymer film used on solar concentrators [9]. The results of the various specular reflectance measurements are shown in Figure 3, which includes a graphical representation of Equation 1. Figure 3 shows specular reflectance readings taken for ReflecTech® Mirror Film that was laminated onto mill-finish aluminum. Mill-finish aluminum is standard grade, low-cost aluminum sheet that is available in sheet form or on coils. The surface of mill-finish aluminum is very good compared to the surface finish of many metals, but there is still some small amount of surface roughness. These surface irregularities can "print through" and impact the specularity of the reflective film that is laminated to the aluminum. A smoother metal surface will improve the specularity.

---

[1] Concentration ratio is sometimes computed as the ratio of the concentrator aperture width divided by the circumference of the absorber tube. To avoid confusion we include the factor of π within the value (e.g. CR = $80/\pi$) when we cite a value for the concentration ratio.
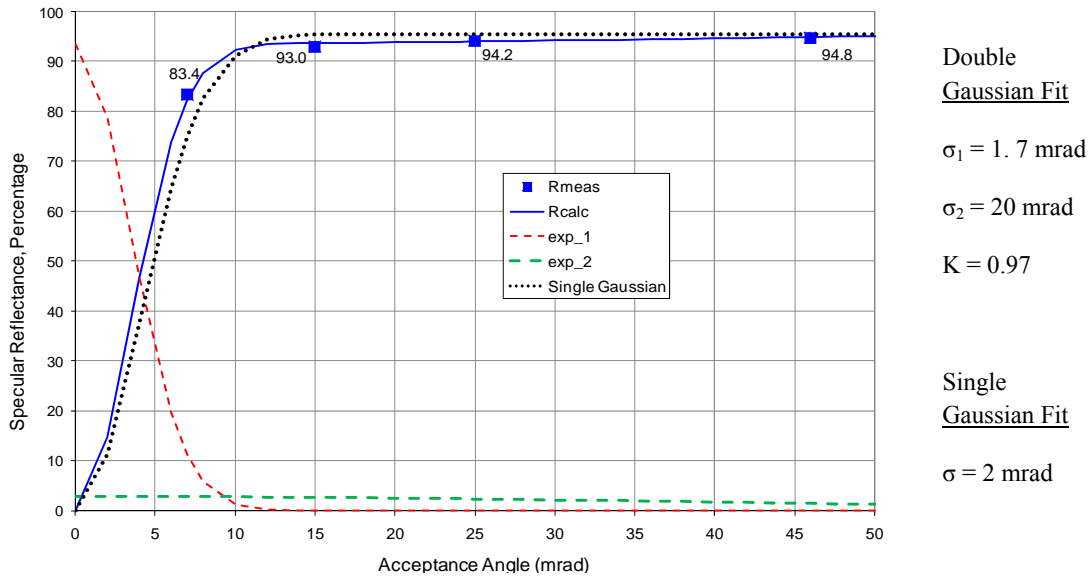
Fig. 3. Specular Reflectance Measurements and Double Gaussian Fit (ReflecTech® on Aluminum)

In Figure 3, the σ_1 and σ_2 Gaussian distributions are shown separately. The dashed red line shows the σ_1 distribution, weighted by K. The green dashed line shows the σ_2 distribution, weighted by (1–K). The solid blue line shows the specular reflectance relationship that results from the double Gaussian fit using equation 1. The specular reflectance measurements at 7, 15, 25 and 46 mrad acceptance angles are the square blue–colored symbols. Note that the four data points are accurately described by the double Gaussian curve fits, indicating that a combination of two Gaussian distributions can accurately describe the distribution of reflected light from a silvered polymer film. The dotted black line is a fit to the data using just a single Gaussian fit, in this case using a σ of 2 mrad. Note that the single Gaussian fit is much less precise compared to the double Gaussian fit. Since the double Gaussian fit is more precise, we incorporate this double Gaussian into our analysis of specularity, as explained in the next section.

3. Analysis Methods

Two optical analysis methods have been used to calculate the impact that specularity has on the optical performance of state-of-the-art parabolic troughs: detailed ray-trace modeling, and a more approximate Gaussian "sum of squares" optical analysis method. The ray trace technique allows precise accounting of optical system affects, but can disguise the functional relationships that exist in an optical system. The "sum of squares" optical analysis method is an approximation, so is less precise, but provides helpful insights into the factors that govern the performance of the optical system, and is easy to use. We have utilized both techniques in order to validate our results as well as to suggest that the simpler method can offer a preferred way of characterizing and assessing a wide variety of reflector surfaces.

3.1. Ray-Tracing Method

The ray-tracing results were computed using a two-dimensional ray-tracing calculation, with the mirror represented by a parabolic arc and the receiver represented by a circle. Each intercept factor reported in this section represents the result of tracing over 3 million rays. We estimate the numerical uncertainty in this calculation to be roughly ±0.1%. These values were computed by a special ray-tracing computation, which allowed representation of individual error terms using first-principle error models which were not necessarily Gaussian.

This calculation method performed several individual ray-tracing calculations assuming perfect conditions, and then combined the resulting output using weighting factors appropriate to particular error assumptions. The core ray-tracing calculations were executed in ASAP, a commercial optical modeling package. Each ASAP calculation assumed perfect optics, a single incident light direction, and a particular receiver position.

To simplify explanation, we will momentarily set aside receiver position error. For a given particular receiver

position, automated software generated an ASAP model for each light direction within a ±30 mrad cone of directions relative to normal incidence, sampled at 0.25 mrad resolution. Executing these models produced a set of output files, each describing the number of rays striking the receiver for the given ray direction.

These results were then combined to compute an intercept factor, using weights specific to each direction. These weights represented the combined influence of sun shape, slope, specularity, tracking, and alignment error. Each was characterized by a distribution appropriate to the specific error source. For example, sun shape was represented by the mean solar brightness profile reported in [10]. Slope error was represented by a Gaussian distribution. Specularity was represented by the dual-Gaussian model described in the previous section. We assume a typical tracking system that operates by moving step-wise through small angle increments; we represent the corresponding angular tracking error as a uniform distribution with width equal to the angle step size. Alignment error is represented by a Gaussian distribution. All of these distributions were represented in a two-dimensional space of angles corresponding to the trough transverse and longitudinal directions. This allowed anisotropic distributions, such as tracking and alignment errors which only apply in the transverse direction. The resulting individual errors were then combined via convolution to produce a distribution representing the combined effect of all angular errors. This final two-dimensional distribution was then projected onto a one-dimensional domain corresponding to the trough transverse direction. The resulting one-dimensional distribution was then used to determine the weighting factors used when combining the results of single-direction ray-trace computations. The resulting weighted combination is an estimate of the intercept factor for this particular receiver position. Note that this estimate is based on non-Gaussian error models for sun shape, specularity, and tracking. These models are quite different from Gaussian assumptions (Figure 4), and more accurately describe their corresponding underlying effects.
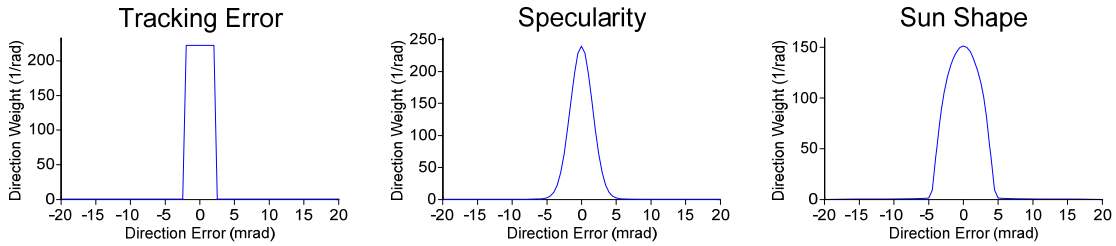

Fig. 4. Non-Gaussian Models used for the Ray-tracing Analysis, after Projection

Finally, this was repeated for a set of different receiver positions, sampled over a ±15 mm range at a 5 mm resolution. The resulting intercept factors were then combined using weights computed from an isotropic two-dimensional Gaussian distribution of receiver positions. The resulting weighted combination produced the final intercept factors. This method was applied to all of the concentration ratio and error scenario entries after modifying the geometry and underlying distributions appropriately for each case.

3.2 Sum-of-Squares Gaussian Approximation Method

The second analysis method that has been used is often referred to as the sum-of-squares method, or the Gaussian approximation method. In this method, all the optical errors are approximated as Gaussian distributions: slope errors of the concentrator, receiver placement errors, tracking errors, the finite size of the sun, twist/misalignment along the length of the collector, and reflector specularity. The total amount of beam spreading is then calculated as the root mean square (rms) value of all the optical errors. This method is described in detail by Bendt, et al [11]. We have used this analysis method, but adapted it to accommodate the specularity term when expressed as a double Gaussian given by Equation 3.

$$\sigma_{total} = \{ 4\sigma_{slope}^2 + \sigma_{rcvr}^2 + \sigma_{track}^2 + \sigma_{sun}^2 + \sigma_{twist}^2 + \sigma_{spec}^2 \}^{1/2} \qquad\qquad (2)$$

$$\text{where } \sigma_{spec}^2 = K\,\sigma_{spec1}^2 + (1-K)\,\sigma_{spec2}^2 \qquad\qquad (3)$$

σ_{slope} = rms angular deviation of concentrator from perfect parabola

σ_{rcvr} = equivalent rms angular spread that accounts for imperfect time-averaged receiver placement

σ_{track} = rms angular spread due to time-averaged sun tracking errors

σ_{sun} = rms angular spread of the sun

σ_{spec} = rms angular spread of reflected beam due to imperfect specularity of the reflector

σ_{twist} = rms angular spread that accounts for imperfect module-to-module alignment of the collector

Summing the optical errors in this way provides a means of characterizing the optical precision of an entire parabolic trough system with a single quantity σ_{total} which can then be used to calculate the optical intercept of the parabolic trough (using Figure 5) with knowledge of the collector geometric concentration ratio and the concentrator rim angle. Because we are primarily interested in high intercept factors, Figure 5 shows only intercept range above 0.9, and rim angles $\geq 60^o$. Figure 5 reproduces the calculations of Bendt, et al; results for rim angles $< 60^o$ are provided in the Bendt reference.

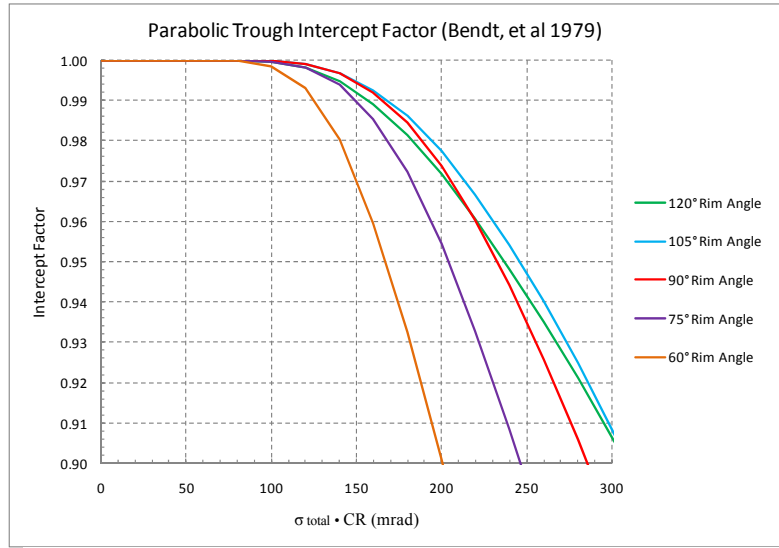**Fig. 5. Intercept Factor vs. ($\sigma_{total} \cdot$ CR) for Different Rim Angles**

Example: Consider a trough with CR = $80/\pi$, a 90° rim angle, σ_{slope} = 3 mrad, σ_{rcvr} = 2 mrad, σ_{track} = 1 mrad, σ_{sun} = 3 mrad, σ_{twist} = 2 mrad, using RefecTech$^{®}$ film laminated onto mill-finish aluminum:

$$\sigma_{spec}^2 = K\,\sigma_{spec1}^2 + (1-K)\,\sigma_{spec2}^2 = 0.97 \cdot 1.7^2 + (1-0.97) \cdot 20^2 = 14.8 \text{ mrad}^2$$

$$\sigma_{total} = \{ 4 \cdot 3^2 + 2^2 + 1^2 + 3^2 + 2^2 + 14.8 \}^{1/2} = (68.8)^{1/2} \text{ mrad} = 8.3 \text{ mrad}$$

So, with CR = $80/\pi$ = 25.5, the product ($\sigma_{total} \cdot$ CR) = 211, and the intercept factor (from Fig 5) is 0.966.

Now, for the purpose of comparison, assume the reflector has perfect specularity. With σ_{spec} = 0 mrad, σ_{total} is reduced to 7.4 mrad, and the intercept factor increases to just above 0.981, a gain of 1.5%.

3.3 Comparison of Two Methods

For the purpose of comparing the detailed ray-tracing results with that of the sum-of-squares Gaussian approximation method, a number of cases were analyzed. We evaluated concentration ratios from $40/\pi$ to $120/\pi$, a range intentionally set well above and well below the norms. We evaluated rms slope errors of 1.75, 3, and 5 mrad. We used $\sigma rcvr$ = 2 mrad, σ_{track} = 0.8 mrad, σ_{twist} = 2 mrad, and σ_{sun} = 3 mrad. The rim angle was 79° for all these comparisons. This choice of rim angle tends to lower the intercept factor (compared to higher rim angles), a characteristic that is clear by inspection of Figure 5. This results in heightened sensitivity to most variables, including specularity, slope errors, etc. This is satisfactory for the purpose of validating that the two calculation methods are comparable. A subset of these cases is shown in Table 1.

Model Parameters	Intercept Factor		
	Ray-Trace	Gaussian	% Difference
CR = 40/π, Ideal reflector, σ_{slope} = 3 mrad	1.000	1.000	0.0%
CR = 40/π, Ideal reflector, σ_{slope} = 5 mrad	0.993	0.996	0.3%
CR = 80/π, Ideal reflector, σ_{slope} = 1.75 mrad	0.993	0.995	0.2%
CR = 80/π, Ideal reflector, σ_{slope} = 5 mrad	0.876	0.876	-0.1%
CR = 120/π, Ideal reflector, σ_{slope} = 1.75 mrad	0.955	0.953	-0.2%
CR = 120/π, Ideal reflector, σ_{slope} = 3 mrad	0.874	0.871	-0.3%
CR = 40/π,, ReflecTech® on aluminum, σ_{slope} = 3 mrad	0.995	1.000	0.5%
CR = 40/π,, ReflecTech® on aluminum, σ_{slope} = 5 mrad	0.986	0.993	0.7%
CR = 80/π, ReflecTech® on aluminum, σ_{slope} = 1.75 mrad	0.980	0.982	0.3%
CR = 80/π, ReflecTech® on aluminum, σ_{slope} = 5 mrad	0.862	0.854	-1.0%
CR = 120/π, ReflecTech® on aluminum, σ_{slope} = 1.75 mrad	0.930	0.902	-3.1%
CR = 120/π, ReflecTech® on aluminum, σ_{slope} = 3 mrad	0.850	0.824	-3.1%

Table 1. Comparison of Intercept Factor Obtained by Ray-Tracing vs. Gaussian Approximation

We have very close agreement for all of the ideal reflector cases, where σ_{spec} was set to zero. The ReflecTech® Mirror Film on aluminum cases also show good agreement for both the low concentration ratio (CR=40/π) and medium concentration ratio (CR=80/π) cases**.** The high concentration ratio (CR=120/π) cases show the largest difference between the ray-trace and Gaussian calculations. We attribute this to the difference between the non-Gaussian detailed models and the simplified Gaussian approximations. Overall, the comparison shows that the sum-of-squares Gaussian approach is a good tool for the purposes of evaluating overall optical performance. The simplicity and calculation speed of this approach has substantial appeal for the purpose of evaluating the optical impact of reflector specularity, especially for low to medium concentration ratios.

4. Results

The sum of squares Gaussian approximation method detailed in the previous sections has been shown to be a good method for evaluating the overall optical impact of specularity. We have used this method to generate the results shown below, and used the double Gaussian approach for characterizing the specularity of ReflecTech® Mirror Film, a commercially available silvered polymeric film for use on solar concentrators.

Figure 6 compares an ideal reflector (i.e. perfect specularity) to a reflector using ReflecTech® Mirror Film. The comparison is made in terms of optical intercept factor for a parabolic trough with a concentration ratio of 80/π that is representative of the utility-scale parabolic trough collectors actively being deployed. This figure shows results at three different levels of slope errors: 1.75 mrad, 3 mrad, and 5 mrad. In all three cases we have made identical assumptions for sun size (σ_{sun} = 3 mrad), tracking errors (σ_{track} = 1 mrad), receiver placement errors (σ_{rcvr} = 2 mrad), and module misalignment errors (σ_{twist} = 2 mrad), and have assumed normal incidence, and a 90° concentrator rim angle.

For the case of a 1.75 mrad rms slope error, the intercept factor assuming perfectly specularity is 0.997. For the 1.75 mrad case using ReflecTech® Mirror Film, the intercept factor is 0.988, which is a 0.9% drop.
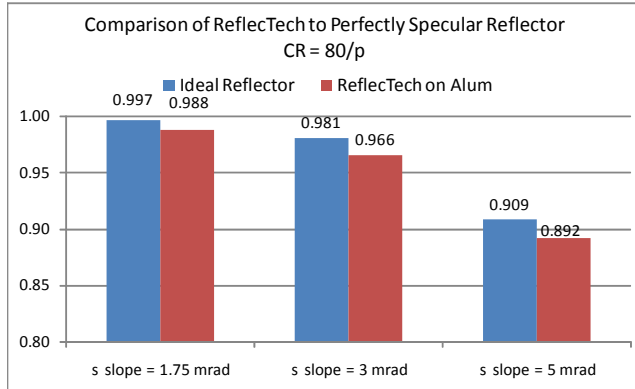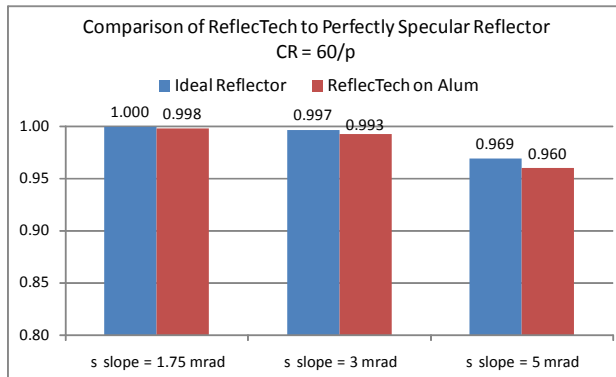
Fig. 6. Intercept Factors for CR=80/π

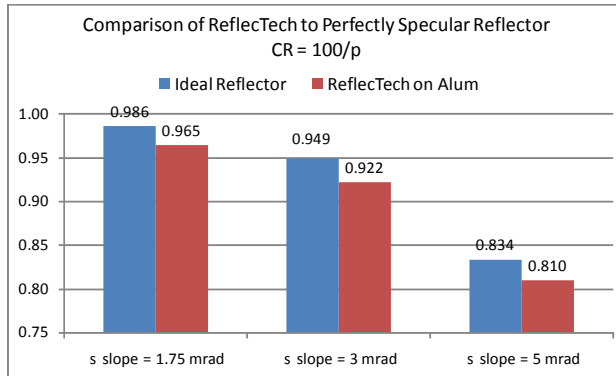**Fig. 7. Intercept Factors for CR=60/π**

Fig. 8. Intercept Factors for CR=100/π

For the 3 mrad rms slope error case, the intercept factor is 0.981, and drops 1.5% to 0.966. This can be considered the baseline case, since a 3 mrad rms slope error is approximately the state of the art for the large glass mirror based collectors that have been recently deployed in the U.S. and in Spain. We note that for this baseline case, the 1.5% loss contrasts markedly with the 5% loss indicated in [1], primarily because that analysis did not account for the entire optical system of a parabolic trough. For the 5 mrad rms slope error case, the intercept factor is 0.909, and drops 1.9% to 0.892. This 5 mrad rms slope error case represents a situation where the slope error is causing a severe loss in optical performance. A proper design solution to reflectors with slope errors in the range of 5 mrad is to lower the concentration ratio.

Figure 7 shows intercept factors when the concentration ratio is lowered to 60/π. Note the 5 mrad slope error case now yields reasonable intercept factors. For all three slope errors (1.75, 3, and 5 mrad), the drop in optical performance from ReflecTech® Mirror Film specularity losses (compared to a perfect reflector) is less than 1%.

Figure 8 shows intercept factors when the concentration ratio is raised to 100/π. Here, the impact of specularity increases, owing to the tighter overall optical precision required to achieve these even higher levels of concentration. The drop in performance due to specularity in these high CR cases is about 2.9%. We also note that slope error is again the primary determinate of intercept factor.

Figure 9 illustrates the relative importance of slope error compared to reflector specularity for parabolic troughs with concentration ratios of 80/π. Over the specularity range of 0 to 4 mrad, the performance impact is about 1.5%. Yet only half that change in slope error (from 2 mrad to 4 mrad), results in a the performance impact ranging from 4 to 5%.

Since slope error of a reflector has a much larger impact than specularity, we examine a special case of interest. The dotted lines in Figure 9 depict the performance drop associated with a specularity of 3.84 mrad (calculated from the "effective Gaussian" using equation 3 for ReflecTech® Mirror Film), compared to a perfectly specular reflective surface. For a concentrator with a 3 mrad rms slope error, the drop in intercept factor (from 0.981 to 0.966) is roughly 1.5%. For the 2 mrad slope error case, the drop is reduced to 1%.

The latter case, the upper dotted line in Fig 9, shows that reducing the slope error from 3 mrad to 2 mrad yields a net gain in performance even when accompanied by a change in specularity from 0 to 3.84 mrad. The ability to achieve this net gain using ReflecTech® Mirror Film has been demonstrated with the reflectors used in the
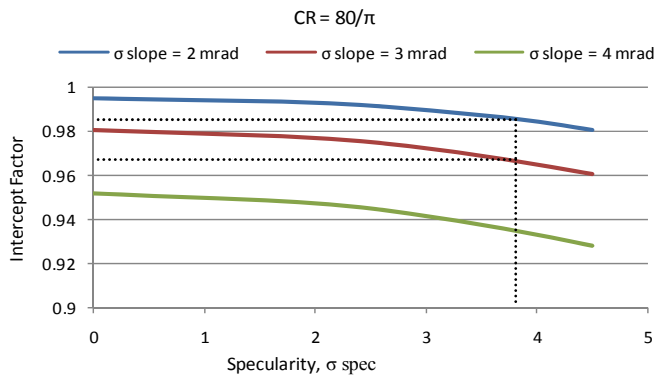
CR = 80/π

— σ slope = 2 mrad   — σ slope = 3 mrad   — σ slope = 4 mrad

Fig. 9. Generalized Optical Impact of Specularity

parabolic concentrator developed at SkyFuel, Inc., which have achieved an rms slope error level of 1.8 mrad [12]. These mirrors are made from continuous panels that span from rim to rim, thus avoiding the inter-mediate free edges and panel-by-panel alignment issues characteristic of other collector designs. The use of reflective film in this design enabled improvements in slope error that more than made up for its reduced specularity.

5. Conclusion

Metalized polymer reflectors are less specular than glass mirrors, and beam spread due to small surface irregularities in polymer reflectors is larger than for glass mirrors. However, when the entire optical system of a parabolic trough is evaluated, this difference in specularity generally leads to a small difference in overall optical performance.

This paper also shows that a reflector surface can be accurately characterized with two fundamental quantities: a) $\rho_{2\pi}$, the solar-weighted hemispherical reflectance, and b) σ_{spec}, the rms of the reflected light distribution which is sometimes best represented as the combination of two Gaussian distributions. By describing the distribution of specularly reflected light (rather than merely counting the light that passes through a particular fixed aperture), σ_{spec} can be used in combination with $\rho_{2\pi}$ to quantitatively, and fairly, compare various parabolic trough reflector surfaces in a way that incorporates the important system-level effects.

References

[1] S. Meyen, E. Lüpfert, J. Pernpeintner, and T. Fend, "Optical Characterisation of Reflector Material for Concentrating Solar Power Technology", SolarPACES 2009 Conference, Sept 15, 2009, Berlin, Germany.

[2] I. Susemihl, P. Schissel, "Specular Reflectance Properties of Silvered Polymer Materials", Solar Energy Materials, volume 16, pg. 403 421, Elsevier Science Publishers, 1987.

[3] W. Short, "Optical Goals for Polymeric Film Reflectors", Solar Energy Research Institute, Golden, CO, SERI/SP-253-3383, Oct 1988.

[4] V. Dudley, et al., "Test Results Industrial Solar Technology Parabolic Trough Solar Collector", Sandia National Laboratories, Albuquerque, NM, SAND--94-1117, November 1995.

[5] A. McMahan, et al., "Field Performance Validation of an Advanced Utility-Scale Parabolic Trough Concentrator", SolarPACES 2010 Conference, Sept. 21, 2010, Perpignon, France.

[6] V. Dudley, et al., "Test Results: SEGS LS-2 Solar Collector", Sandia National Laboratories, Albuquerque, NM, SAND94-1884, December 1994.

[7] G. Cohen, "A CSP Industry Point of View of DOE'S Systems –Driven Approach", Solar Energy Systems Symposium , Sandia National Laboratories, Albuquerque NM, October 15-17 , 2003.

[8] R. Petitt, et al. "Simplified Calculational Procedure for Determining the Amount of Intercepted Sunlight in an Imaging Solar Concentrator", J. Sol. Energy Eng., Volume 105, Issue 1, 101 February 1983.

[9] M. DiGrazia, et al. "ReflecTech Mirror Film Attributes and Durability for CSP Applications", Proceedings of ES2009 Energy Sustainability 2009, July 19-23, 2009, San Francisco, California USA.

[10] A. Neumann, et al. "Representative Terrestrial Solar Brightness Profiles", Journal of Solar Energy Engineering Vol. 124, May 2002.

[11] P. Bendt, A. Rabl, H. Gaul, and K. Reed, "Optical Analysis and Optimization of Line-Focus Solar Collectors, Solar Energy Research Institute, Golden, CO, SERI/TR 34-092, Sept 1979.

[12] R. Brost, A. Gray, F. Burkholder, T. Wendelin, D. White, "SkyTrough Optical Evaluations Using VSHOT Measurement", SolarPACES 2009 Conference, Sept 15, 2009, Berlin, Germany.